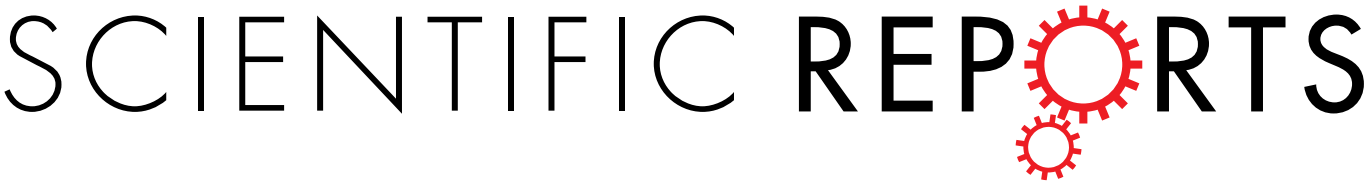

OPEN

Optimal architectures for long distance quantum communication

Sreraman Muralidharan[1,*], Linshu Li[2,*], Jungsang Kim[3], Norbert Lütkenhaus[4], Mikhail D. Lukin[5] & Liang Jiang[2]

Received: 09 November 2015
Accepted: 04 January 2016
Published: 15 February 2016

Despite the tremendous progress of quantum cryptography, efficient quantum communication over long distances (≥1000 km) remains an outstanding challenge due to fiber attenuation and operation errors accumulated over the entire communication distance. Quantum repeaters (QRs), as a promising approach, can overcome both photon loss and operation errors, and hence significantly speedup the communication rate. Depending on the methods used to correct loss and operation errors, all the proposed QR schemes can be classified into three categories (generations). Here we present the first systematic comparison of three generations of quantum repeaters by evaluating the cost of both temporal and physical resources, and identify the optimized quantum repeater architecture for a given set of experimental parameters for use in quantum key distribution. Our work provides a roadmap for the experimental realizations of highly efficient quantum networks over transcontinental distances.

First developed in the 1970s, fiber-optic communication systems have boosted the rate of classical information transfer and played a major role in the advent of the information age. The possibility to encode information in quantum states using single photons and transmit them through optical channels has led to the development of quantum key distribution (QKD) systems[1]. However, errors induced by the intrinsic channel attenuation, i.e. loss errors, become a major barrier for efficient quantum communication over continental scales, due to the exponential decay of communication rate[2]. In contrast to classical communication, due to the quantum no-cloning theorem[3], quantum states of photons cannot be amplified without any disturbance. In addition to loss errors, depolarization errors introduced by the imperfect optical channel can impair the quality of the single photon transmitted and hence the quantum information encoded.

To overcome these challenges, quantum repeaters (QRs) have been proposed for the faithful realization of long-distance quantum communication[4]. The essence of QRs is to divide the total distance of communication into shorter intermediate segments connected by QR stations, in which loss errors from fiber attenuation can be corrected. Active mechanisms are also employed at every repeater station to correct operation errors, i.e. imperfections induced by the channel, measurements and gate operations.

As illustrated in Fig. 1, loss errors can be suppressed by either heralded entanglement generation (HEG)[4,5] or quantum error correction (QEC)[6–10]. During HEG, quantum entanglement can be generated with techniques such as two-photon interference conditioned on the click patterns of the detectors in between. Loss errors are suppressed by repeating this heralded procedure until the two adjacent stations receive the confirmation of certain successful detection patterns via *two-way* classical signaling.

Alternatively, one may encode the logical qubit into a block of physical qubits that are sent through the lossy channel and use quantum error correction to restore the logical qubit with only *one-way* signaling. Quantum error correcting codes can correct no more than 50% loss rates deterministically due to the no-cloning theorem[9,11]. To suppress operation errors, one may use either heralded entanglement purification (HEP)[12,13] or QEC[6–10] as listed in Fig. 1. In HEP, multiple low-fidelity Bell pairs are consumed to probabilistically generate a smaller number of higher-fidelity Bell pairs. Like HEG, to confirm the success of purification, *two-way* classical signaling between repeater stations for exchanging measurement results is required. Alternatively, QEC can correct operation errors using only *one-way* classical signaling, but it needs high fidelity local quantum gates.

Based on the methods adopted to suppress loss and operation errors, we can classify various QRs into three categories as shown schematically in Fig. 2, which we refer to as three generations of QRs[14]. Note that the

[1]Department of Electrical Engineering, Yale University, New Haven, CT 06511 USA. [2]Department of Applied Physics, Yale University, New Haven, CT 06511 USA. [3]Department of Electrical and Computer Engineering, Duke University, Durham, NC 27708 USA. [4]Institute of Quantum computing, University of Waterloo, N2L 3G1 Waterloo, Canada. [5]Department of Physics, Harvard University, Cambridge, MA 02138, USA. *These authors contributed equally to this work. Correspondence and requests for materials should be addressed to L.J. (email: liang.jiang@yale.edu)

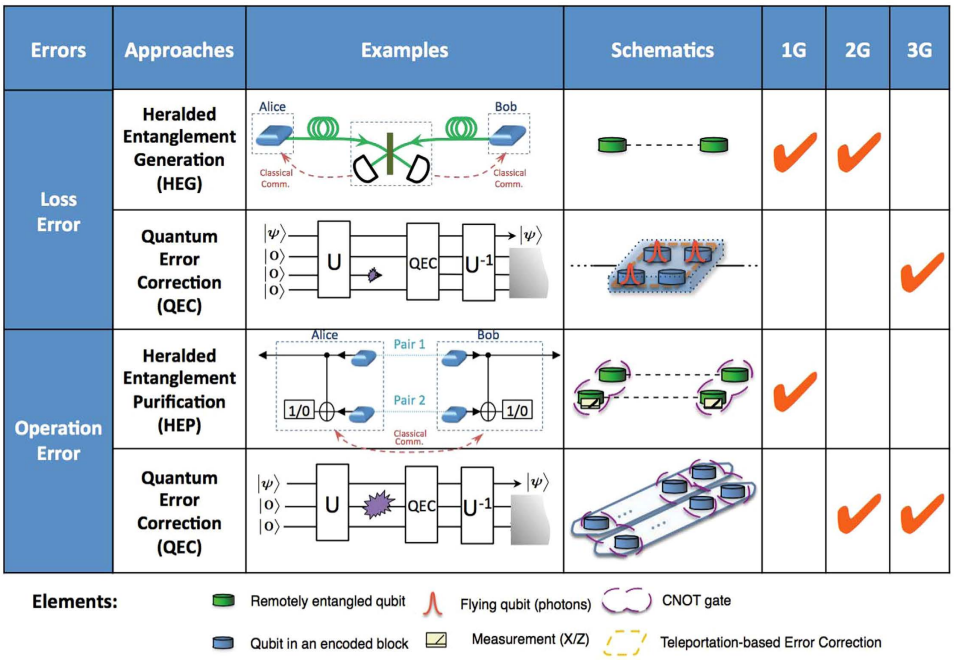

Figure 1. A list of methods to correct loss and operation errors. Depending on the methods used to correct the errors, QRs are categorized into three generations.

	First Generation QR	Second Generation QR	Third Generation QR
Schematic Architecture	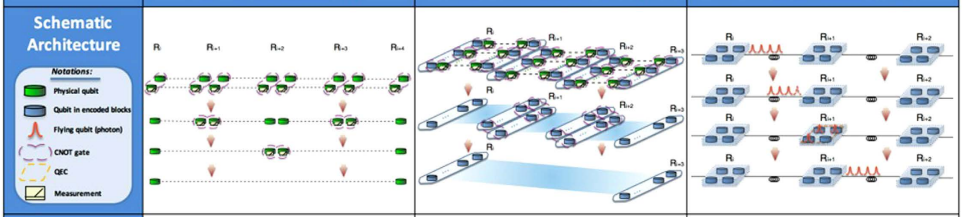		
Loss Error	HEG (two-way signaling)	HEG (two-way signaling)	QEC (one-way signaling)
Operation Error	HEP (two-way signaling)	QEC (one-way signaling)	QEC (one-way signaling)
Procedure	1. Create entangled pairs over L_0 between adjacent stations 2. At k-th level, connect two pairs over L_k and extend to $L_{k+1}=2L_k$, followed by HEP. 3. After n nesting levels, obtain high-fidelity pair over $L_{tot}=2^n \times L_0$	1. Prepare encoded states $\|0\rangle_L$ and $\|+\rangle_L$ 2. Use teleportation-based non-local CNOT gates to create encoded Bell pairs between adjacent stations. 3. Connect intermediate stations to create long distance encoded Bell pair	1. Encode information with a block of qubits that are sent through a lossy channel 2. Use QEC to correct both loss and operation errors 3. Relay the encoded information to the next station; and repeat steps 2 & 3.
Characteristic time scale	$\mathrm{Max}(L_{tot}/c, t_0)$	$\mathrm{Max}(L_0/c, t_0)$	t_0
Cost Coefficient (C')	$\mathrm{Poly}(L_{tot})$	$\mathrm{PolyLog}(L_{tot})$	$\mathrm{PolyLog}(L_{tot})$

Figure 2. Comparison of three generations of QRs.

combination of QEC for loss errors and HEG for operation errors is sub-optimum compared to the other three combinations.

Each generation of QR performs the best for a specific regime of operational parameters such as local gate speed, gate fidelity, and coupling efficiency. We consider both the temporal and physical resources consumed by the three generations of QRs and identify the most efficient architecture for different parameter regimes. The results can guide the design of efficient long distance quantum communication links that act as elementary building blocks for future quantum networks.

In this paper, we will first briefly review the chacracterstics of three generations of QRs. We use the cost coefficient as an optimization metric to compare the QR performance, and study its dependence on the individual operational parameters including coupling efficiency, gate speed and gate fidelity. Later, we present a holistic view

of the optimization and illustrate the parameter regions where each generation of QRs performs more efficiently than others. Finally, we analyze the advantages and challenges of each generation of QRs and discuss the experimental candidates for their realizations.

Results

Three generations of quantum repeaters. The first generation of QRs uses HEG and HEP to suppress loss and operation errors, respectively[4,5]. This approach starts with purified high-fidelity entangled pairs with separation $L_0 = L_{tot}/2^n$ created and stored in adjacent stations. At k-th nesting level, two entangled pairs of distance $L_{k-1} = 2^{k-1}L_0$ are connected to extend entanglement to distance $L_k = 2^k L_0$[15]. As practical gate operations and entanglement swapping inevitably cause the fidelity of entangled pairs to drop, HEP can be incorporated at each level of entanglement extension[12,13]. With n nesting levels of connection and purification, a high-fidelity entangled pair over distance $L_n = L_{tot}$ can be obtained. The first generation of QRs reduces the exponential overhead in direct state transfer to only polynomial overhead, which is limited by the two-way classical signaling required by HEP between non-adjacent repeater stations. The communication rate still decreases polynomially with distance and thus becomes very slow for long distance quantum communication. The communication rate of the first generation of QRs can be boosted using temporal, spatial, and/or frequency multiplexing associated with the internal degrees of freedom for the quantum memory[5,16].

The second generation of QRs uses HEG to suppress loss errors and QEC to correct operation errors[6,7,17]. First, the encoded states $|0\rangle_L$ and $|+\rangle_L$ are fault-tolerantly prepared using the Calderbank-Shor-Steane (CSS) codes and stored at two adjacent stations. CSS codes are considered because of the fault tolerant implementation of preparation, measurement, and encoded CNOT gate[6,18]. Then, an encoded Bell pair $|\Phi^+\rangle_L = \frac{1}{\sqrt{2}}\left(|0,0\rangle_L + |1,1\rangle_L\right)$ between adjacent stations can be created using teleportation-based non-local CNOT gates[19,20] applied to each physical qubit in the encoded block using the entangled pairs generated through HEG process. Finally, QEC is carried out when entanglement swapping at the encoded level is performed to extend the range of entanglement. The second generation uses QEC to replace HEP and therefore avoids the time-consuming two-way classical signaling between non-adjacent stations. The communication rate is then limited by the time delay associated with two-way classical signaling between adjacent stations and local gate operations. If the probability of accumulated operation errors over all repeater stations is sufficiently small, we can simply use the second generation of QRs *without* encoding.

The third generation of QRs relies on QEC to correct both loss and operation errors[8–10,21]. The quantum information can be directly encoded in a block of physical qubits that are sent through the lossy channel. If the loss and operation errors are sufficiently small, the received physical qubits can be used to restore the whole encoding block, which is retransmitted to the next repeater station. The third generation of QRs only needs *one-way* signaling and thus can achieve very high communication rate, just like the classical repeaters only limited by local operation delay. It turns out that quantum parity codes[22] with moderate coding blocks (200 qubits) can efficiently overcome both loss and operation errors[9,21].

Note that the second and third generations of QRs can achieve communication rate much faster than the first generation over long distances, but they are technologically more demanding. For example, they require high fidelity quantum gates as QEC only works well when operation errors are below the fault tolerance threshold. The repeater spacing for the third generation of QRs is smaller compared to the first two generation of QRs because error correction can only correct a finite amount of loss errors. Moreover, quantum error correcting codes can correct only up to 50% loss error rates deterministically, which restricts the applicable parameter range for the third generation of QRs[9].

Besides quantum key distribution, QRs can also be used for quantum state transfer. The resource requirement is mostly unchanged for the first and third generations of QRs. For the second generation, however, additional long-lived quantum memories will be required at the end (receiver) station, because the receiver has to wait for and collect all the classical signals to complete quantum teleportation.

Comparison of three generations of QRs. To present a systematic comparison of different generations in terms of efficiency, we need to consider both temporal and physical resources. The temporal resource depends on the rate, which is limited by the time delay from the two-way classical signaling (first and second generations) and the local gate operation (second and third generations, see details below)[23]. The physical resource depends on the total number of qubits needed for HEP (first and second generations) and QEC (second and third generations)[9,24]. We propose to quantitatively compare the three generations of QRs using a cost function[9] related to the required number of qubit memories to achieve a given transmission rate. Suppose a total of N_{tot} qubits are needed to generate secure keys at R bits/second, the cost function is defined as

$$C(L_{tot}) = \frac{N_{tot}}{R} = \frac{N_s}{R} \times \frac{L_{tot}}{L_0}, \tag{1}$$

where N_s is the number of qubits needed per repeater station, L_{tot} the total communication distance, and L_0 the spacing between neighboring stations. Since the cost function scales at least linearly with L_{tot}, to demonstrate the additional overhead associated with L_{tot}, the *cost coefficient* can be introduced as

$$C'(L_{tot}) = C/L_{tot}, \tag{2}$$

which can be interpreted as the resource overhead (qubits × time) for the creation of one secret bit over 1 km (with target distance L_{tot}). Besides the fiber attenuation (with $L_{att} = 20$ km for telecom wavelengths), the cost

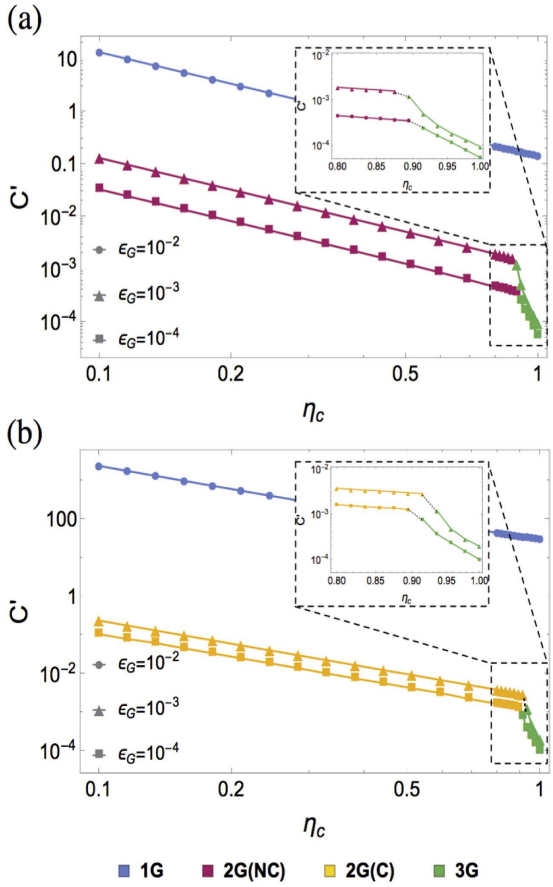

Figure 3. The optimized cost coefficient C' as a function of η_c for $t_0 = 1\,\mu s$, $\varepsilon_G \in \{10^{-2}, 10^{-3}, 10^{-4}\}$, and **(a)** $L_{tot} = 1000$ km, (**b**) $L_{tot} = 10{,}000$ km. The associated optimized QR protocols are indicated in different colors 2G(NC) and 2G(C) correspond to second generation without and with encoding, respectively.

coefficient also depends on other experimental parameters, in particular the coupling efficiency η_c (see supplementary material), the gate error probability ε_G, and the gate time t_0. For simplicity, we make the following assumptions. 1) We assume that the fidelity of physical Bell pairs $F_0 = 1 - \frac{5}{4}\varepsilon_G$ achieved with entanglement purification and measurement error probability $\varepsilon_m = \frac{\varepsilon_G}{4}$ through a verification procedure (See supplementary material). 2) For third generation QRs, we restrict the search only up to 200 qubits per logical qubit considering the complexity involved in the production of larger codes and for a fair comparison with second generation of QRs. 3) We will assume that t_0 is independent of code size for small encoded blocks for second and third generation QRs. We will now investigate how C' varies with these parameters for three generations of QRs, and identify the optimum generation of QR depending on the technological capability.

Coupling efficiency. The coupling efficiency η_c accounts for the emission of photon from the memory qubit, coupling of the photon into the optical fiber and vice versa, and the final detection of photons. The first and second generations of QRs use HEG compatible with arbitrary coupling efficiency, while the third generation relies on QEC requiring the overall transmission (including the coupling efficiency η_c and the channel transmission) to be at least above 50%[9,25]. As illustrated in Fig. 3, for high coupling efficiency ($\eta_c \gtrsim 90\%$) the third generation of QRs has an obvious advantage over the other generations due to the elimination of two-way classical signaling. As the coupling efficiency is reduced and approaches (~90%) for quantum parity codes, the size of the coding block quickly increases and it becomes less favorable to use this approach. For coupling efficiency below ~90%, the optimization chooses the first and second generations of QRs, and then C' is proportional to η_c^{-2} for HEG protocols heralded by two-photon detector click patterns.

If the gate error becomes large (e.g., $\varepsilon_G = 10^{-2}$), the capability of correcting loss errors will be compromised for the third generation QRs. Similar trends can be observed as we fix ε_G and increase L_{tot}. In contrast to the third generation QRs, the first and second generation QRs with HEG works well even for low coupling efficiencies.

Speed of quantum gates. We investigate the performance of different generations of QRs for different gate times in the range $0.1\,\mu s \leq t_0 \leq 100\,\mu s$. As shown in Fig. 4, for high speed quantum gates ($t_0 \lesssim 1\,\mu s$) the third generation of QRs provides a very fast communication rate, which makes it the most favorable protocol, with $C' \propto t_0$. For slower quantum gates ($t_0 \gtrsim 10\,\mu s$), the gate time becomes comparable or even larger than the delay of two-way

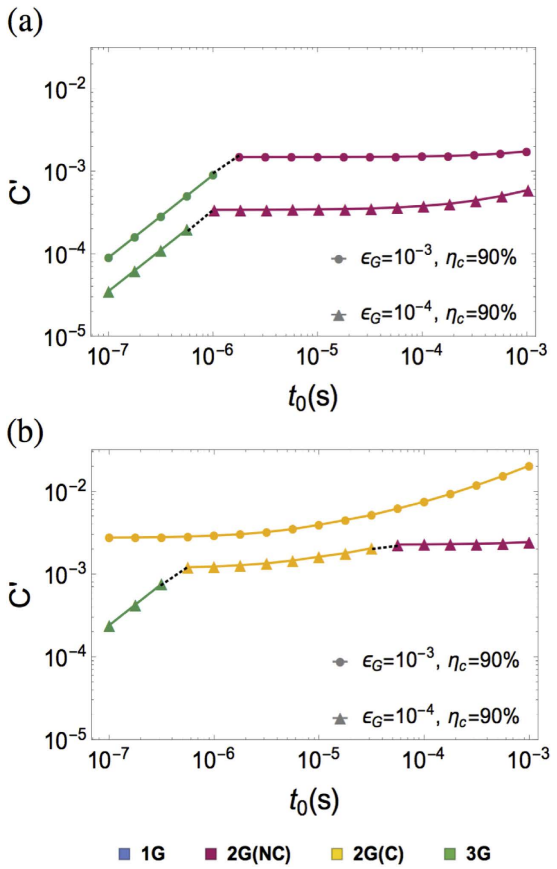

Figure 4. The optimized cost coefficient C' as a function of t_0 for $\eta_c = 0.9$, $\varepsilon_G \in \{10^{-3}, 10^{-4}\}$, and **(a)** $L_{tot.} = 1000$ km, (**b**) $L_{tot.} = 10{,}000$ km. The associated optimized QR protocols are indicated in different colors.

classical signaling between adjacent stations $\left(t_0 \gtrsim \frac{L_0}{c} \approx \frac{L_{att}}{c}\right)$; as the third generation of QRs loses its advantage in communication rate, the second generation of QRs with less physical resources becomes the optimized QR protocol, with almost constant C' for a wide range of t_0.

We notice that for small gate error and intermediate distance (e.g., $\varepsilon_G = 10^{-4}$ and $L_{tot} = 1000$ km appeared in Figs 3a and 4a), encoding might not even be necessary for the second generation of QRs, because the accumulated errors over the entire repeater network are within the tolerable range for quantum communication $\left(\varepsilon_G \frac{L_{tot}}{L_{att}} \lesssim 0.1\right)$. However, for larger error probability or longer distances $\left(\varepsilon_G \frac{L_{tot}}{L_{att}} \gg 0.1\right)$, encoding is required for the second generation QRs. When ε_G increases from 10^{-4} to 10^{-3}, the cost coefficient for the second generation of QR without encoding increases by almost a factor of 10 (Fig. 4a), while the change is less significant for the second and third generations of QRs with encoding (Fig. 4). This is because at the logical level, the change in the effective logical error probability is suppressed for the given set of parameters. The cost coefficient for the first generation of QRs $\left(C' > 1 \frac{qubit \times sec}{sbit \times km}\right)$ lies beyond the scope of Fig. 4, with little dependence on t_0 that is mostly negligible compared to the two-way classical signaling between non-adjacent stations $\left(\frac{L_{tot}}{c} > 10ms\right)$.

Gate fidelity. The three generations of QRs have different thresholds in terms of gate error probability ε_G. The first generation relies on HEP with the highest operation error threshold up to about 3%[4]. The second and third generations both use QEC to correct operation errors, with error correction thresholds of approximately 1%[26]. The gate error threshold of the second generation is slightly lower than that of the third generation, because of the extra gates required for teleportation-based non-local CNOT gates and entanglement swapping in the second generation of QRs (See supplementary material). However, since we restrict the size of the encoded block for third generation of QRs, C' increases exponentially with ε_G slightly below the theoretical threshold of quantum parity codes. As illustrated in Fig. 5, for almost perfect coupling efficiency (e.g. $\eta_c = 100\%$) and fast local operation ($t_0 = 1\,\mu s$), the third generation using QEC to correct both fiber attenuation loss and operation errors is the optimized protocol for moderate gate errors. For lower coupling efficiencies (e.g. $\eta_c = 30\%$ and 80%) with too many loss errors for the third generation to tolerate, the first and second generations with HEG yield good performance. As ε_G increases, there is a transition at about 0.8% (0.6%) below which the second generation is more favorable for 1000 km (10000 km).

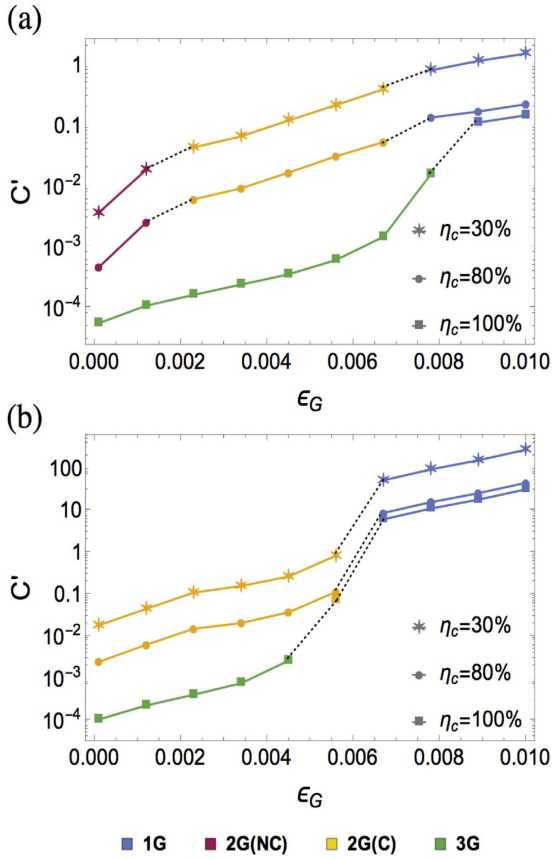

Figure 5. The optimized cost coefficient C′ as a function of ε_G for $t_0 = 1\,\mu s$, $\eta_c \in \{30\%, 80\%, 100\%\}$, and (**a**) $L_{tot} = 1000$ km, (**b**) $L_{tot} = 10{,}000$ km. The associated optimized QR protocols are indicated in different colors.

Optimum generation of QRs. Based on the above analysis of the cost coefficient that depends on the coupling efficiency η_c, the gate time t_0, and the gate infidelity ε_G, we may summarize the results using the bubble plot and the region plot in the three-dimensional parameter space, as shown in Fig. 6. The bubble color indicates the associated optimized QR protocol, and the bubble diameter is proportional to the cost coefficient. The parameter space can be divided into the following regions: (I) For high gate error probability ($\varepsilon_G \gtrsim 1\%$), the first generation dominates; (II.A) For intermediate gate error probability, but poor coupling efficiency or slow local operation [$0.1\frac{L_{att}}{L_{tot}} \lesssim \varepsilon_G \lesssim 1\%$ and ($\eta_c \lesssim 90\%$ or $t_0 \gtrsim 1\,\mu s$)], the second generation *with* encoding is more favorable; (II.B) For low gate error probability, but low coupling efficiency or slow local operation [$\varepsilon_G \lesssim 0.1\frac{L_{att}}{L_{tot}}$ and ($\eta_c \lesssim 90\%$ or $t_0 \lesssim 1\,\mu s$)], the second generation *without* encoding is more favorable; (III) For high coupling efficiency, fast local operation, and low gate error probability ($\eta_c \gtrsim 90\%$, $t_0 \lesssim 1\,\mu s$, $\varepsilon_G \lesssim 1\%$), the third generation becomes the most favorable scheme in terms of the cost coefficient.

Discussion

So far, we have mostly focused on the standard procedure of HEG and HEP[4,5,12,13], the CSS-type quantum error correcting codes, and the teleportation-based QEC, which all can be improved and generalized. We have also assumed the simple cost function that scales linearly with the communication time and the total number of qubits. In practice, however, the cost function may have a more complicated dependence on various resources. Nevertheless, we may extend our analysis by using more realistic cost functions to compare various QR protocols. As we bridge the architectural design of QRs and the physical implementations, we may include more variations of HEG, HEP as well as QEC and use more realistic cost functions, while the general trend and different parameter regions should remain mostly insensitive to these details. Recently, there have been growing interest in all optical quantum repeaters[14,27,28] which does not require memory qubits. In such cases, the cost coefficient can be naturally extended to key generation rate/mode[2] (in units bits/second/mode) and one can consider its maximization to compare different QR schemes.

The classification of QR protocols with different performance in the parameter space also provides a guideline for optimized architectural design of QRs based on technological capabilities, which are closely related to physical implementations, including atomic ensembles, trapped ions, NV centers, quantum dots, nanophotonic devices, etc. (1) The atomic ensemble can be used as quantum memory with high coupling efficiency (>80%[29,30]) and compatible with HEG for the first generation of QRs[31]. An important challenge for ensemble-based QRs is the use of non-deterministic quantum gates, which can be partly compensated by *multiplexing* various internal

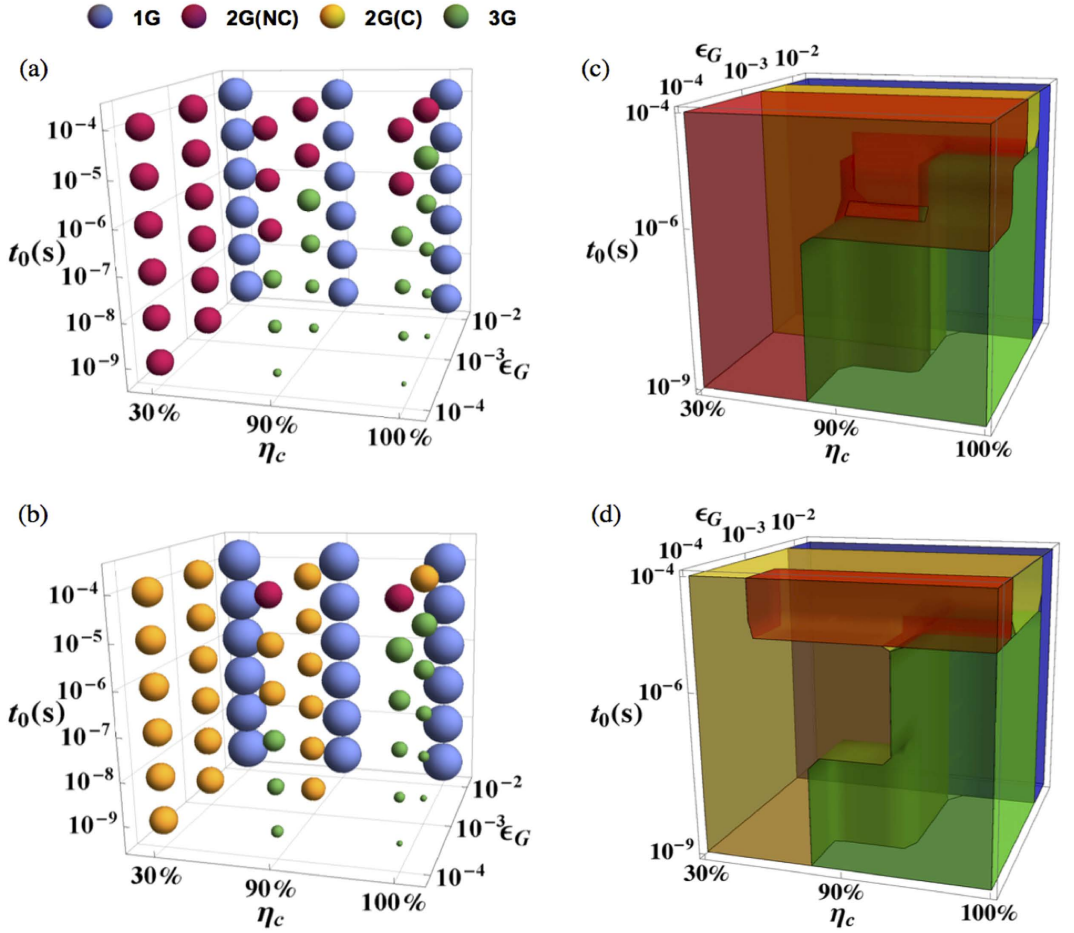

Figure 6. The bubble plot comparing various QR protocols in the three-dimensional parameter space spanned by η_c, ε_G, and t_0, for **(a)** $L_{tot} = 1000$ km and (**b**) $L_{tot} = 10{,}000$ km. The bubble color indicates the associated optimized QR protocol, and the bubble diameter is proportional to the cost coefficient. The region plots (**c**,**d**) showing the distribution of different optimized QR protocol in the three dimensional parameter space for $L_{tot} = 1000$ km and $L_{tot} = 10{,}000$ km respectively. The region plot (**c**) contains a yellow region of second generation with encoding, which can be verified in a bubble plot with a finer discretization of ε_G.

modes of the ensemble memory[5,16]. Alternatively, the atomic ensemble approach can be supplemented by deterministic atom-photon and atom-atom gates using Rydberg blockade, which can dramatically improve the performance of atomic ensemble approaches and make them compatible with both first and second generations of QRs[32,33]. (2) The trapped ions, NV centers, and quantum dots all can implement local quantum operations deterministically[34–38], as well as HEG[39–42]. In principle, they are all compatible with the first and second generations of QRs. Although the coupling efficiency is relatively low for single emitters compared to ensembles, it can be boosted with cavity Purcell enhancement[43] (by two orders of magnitude). With high coupling efficiency[44,45], these systems can also be used for the third generation of QRs. (3) The system of nanophotonic cavity with individual trapped neutral atoms has recently demonstrated quantum optical switch controlled by a single atom with high coupling efficiency[46,47], which can be used for deterministic local encoding and QEC for the third generation of QRs. Realization of similar techniques with atom-like emitters are likewise being explored. (4) The opto-electro-mechanical systems have recently demonstrated efficient coherent frequency conversion between optical and microwave photons[48,49] and can potentially enable using superconducting systems[50] for reliable fast local quantum gates for QRs.

In conclusion, we have classified various QR protocols into three generations based on different methods for suppressing loss and operation errors. Introducing the cost function to characterize both temporal and physical resources, we have systematically compared three generations of QRs for various experimental parameters, including coupling efficiency, gate time and gate fidelity. There are different parameter regions with drastically different architectural designs of quantum repeaters with different possible physical implementations. Our work will provide a guideline for the optimal design of quantum networks and help in the extension of quantum network of clocks[51], interferometric telescopes[52] and distributed quantum computation[20,53] to global scales. In the future, the integration of different generations of QRs will enable the creation of a secure quantum internet[54].

Methods

Descriptions of error models. Local two-qubit gates, e.g. CNOT gate, are characterized by the gate infidelity ε_G. With probability $1-\varepsilon_G$ the desired two-qubit gate is applied, while with probability ε_G the state of the two qubits becomes a maximally mixed state. Mathematically the imperfect two-qubit operation on qubit i and j can be expressed as

$$U\rho U^{\dagger} = (1-\varepsilon_G)\, U_{ij}\rho U_{ij}^{\dagger} + \frac{\varepsilon_G}{4} Tr_{ij}[\rho] \otimes I_{ij}, \tag{3}$$

where U_{ij} stands for perfect two-qubit operation on qubit i and j, $Tr_{ij}[\rho]$ the partial trace over qubit i and j, and I_{ij} the identity operator for qubits i and j.

Qubit measurement error is described by the measurement infidelity ξ, which is the probability of a wrong measurement. The error models for projective measurements of states $|0\rangle$ and $|1\rangle$ are

$$\begin{aligned} P_0 &= (1-\xi)\,|0\rangle\langle 0| + \xi|1\rangle\langle 1| \\ P_1 &= (1-\xi)\,|1\rangle\langle 1| + \xi|0\rangle\langle 0|. \end{aligned} \tag{4}$$

The measurement error can be suppressed by introducing an ancillary qubit for measurement and measuring both the data and the ancillary qubits. If the measurement outcomes don't match, it can be considered as a loss error on that qubit. The contribution of the measurement error to the overall loss error is negligible given the range of the gate error rates (10^{-4}–10^{-2}) we are considering; if they match, then the effective measurement error is given by $\frac{\varepsilon_G}{4}$[26].

In the calculations, the memory qubits are assumed to be perfect, i.e. their life-time is tremendously longer than any characteristic times involved in each scheme. In this sense the most demanding scheme is the first generation, which is optimum at long communication distances, e.g. $L_{tot} = 10^4$ km, and high gate errors. The required coherence time τ for memory qubits is at least limited by the fundamental two-way classical communication time between Alice and Bob

$$t_{c1} = \frac{L_{tot}}{c} \sim 50ms, \tag{5}$$

where $c = 2\times 10^5$ km/s is the speed of light in telecom-wavelength optical fiber. Recent experiments with trapped ions, superconducting qubits, solid state spins and neutral atoms have demonstrated quantum memory life-times approaching or exceeding this characteristic value. For the second generation, the characteristic communication time is

$$t_{c2} = \frac{L_{att}}{c} \sim 100\,\mu s \tag{6}$$

where $L_{att} = 20$ km at telecomm wavelength. The corresponding coherence times are far less demanding than that of the first generation, which relieves the strong life-time requirements on memory qubits and makes the two generations more plausible in practice. Note that when the operation time t_0 becomes comparable or larger than the characteristic communication time, it is then the operation time t_0 that puts limits to the coherence time τ. Third generation QRs are not limited by the two way communication time because it is a fully one way communication scheme.

Entanglement fidelity and entanglement purification. The density matrix of an imperfect Bell pair can be expressed in the Bell basis as the following

$$\rho = a|\varphi^+\rangle\langle\varphi^+| + b|\varphi^-\rangle\langle\varphi^-| + c|\psi^+\rangle\langle\psi^+| + d|\psi^-\rangle\langle\psi^-|, \tag{7}$$

where $|\varphi^{\pm}\rangle = \frac{1}{\sqrt{2}}(|00\rangle \pm |11\rangle)$ and $|\psi^{\pm}\rangle = \frac{1}{\sqrt{2}}(|01\rangle \pm |10\rangle)$ are the four Bell states. The fidelity of the pair is thus defined as

$$F \equiv a = \langle\varphi^+|\rho|\varphi^+\rangle, \tag{8}$$

Both the first and second generations of QRs rely on generating elementary entangled pairs between neighboring repeater stations and then extending the entanglement to longer distances. Practically, however, an entangled pair generated between neighboring stations may not be a perfect Bell pair. In addition, for the first generation, HEP is needed at higher levels of entanglement extension to overcome operation errors. With the technique of HEP, the fidelity of entangled pairs can be boosted to near-unity at the cost of reducing the total number of them and purified pairs can be connected to obtain longer entangled pairs or used as resources for implementing remote quantum gates.

We note that with imperfect quantum operations and measurements, there is an upper bound on the fidelity of entangled pairs even with entanglement purification. It is in general, a function of the density matrix of raw Bell pairs ρ, gate infidelity ε_G and measurement infidelity ξ, and depends on the specific purification protocol one uses. Using Deutsch *et al.* purification protocol (see the supplementary for details), the value of this upper bound can be approximated as

$$F_{u.b.} = 1 - \frac{5}{4}\varepsilon_G - \left(\frac{9}{4}\xi + \frac{19}{4}\varepsilon_G\right)\varepsilon_G + \mathcal{O}(\varepsilon_G,\xi)^3 \approx 1 - \frac{5}{4}\varepsilon_G, \quad (9)$$

in which we assume depolarized states for input raw Bell pairs. This approximate expression holds at small ε_G's ($\lesssim$1%). In our calculations and comparison, the temporal resources and physical resources consumed in obtaining purified pairs between neighboring stations are not accounted; elementary entangled pairs generated between neighboring stations are assumed to directly take this asymptotic value. The associated additional cost in the purification can be easily added as an overhead into the cost function.

For HEP at higher levels in the first generation, we consider two widely used entanglement purification protocols: Deutsch *et al.* protocol[12] and Dür[13] *et al.* protocol. Compared to other purification schemes, the Deutsch protocol reaches higher fidelities with fewer rounds of purification so its upper bound is used as the fidelity of elementary pairs between neighboring stations. The Dür *et al.* purification protocol is very similar to the Deutsch *et al.* protocol, except that one of the two pairs, called auxiliary pair, is never discarded and will be prepared in the same state in each round of purification. This is sometimes also call "entanglement pumping". The Dür *et al.* purification protocol saves qubit resources by keeping making use of the auxiliary pair, while the state preparation in each purification round is costly in time as a trade-off and if one round fails, the whole purification needs to be started over again. Details of the two protocols can be found in the supplementary. Note that, in general, despite differences in experimental requirements and efficiencies, the choice of purification protocols will not affect the big picture of scheme optimization.

References

1. Lo, H.-K., Curty, M. & Tamaki, K. Secure quantum key distribution. *Nature Photon* **8,** 595–604 (2014).
2. Takeoka, M., Guha, S. & Wilde, M. M. Fundamental rate-loss tradeoff for optical quantum key distribution. *Nature comm.* **5,** 5235 (2014).
3. Wootters, W. K. & Zurek, W. H. A single quantum cannot be cloned. *Nature* **299,** 802–803 (1982).
4. Briegel, H.-J., Dür, W., Cirac, J. & Zoller, P. Quantum Repeaters: The Role of Imperfect Local Operations in Quantum Communication. *Phys. Rev. Lett.* **81,** 5932–5935 (1998).
5. Sangouard, N., Simon, C., de Riedmatten, H. & Gisin, N. Quantum repeaters based on atomic ensembles and linear optics. *Rev. Mod. Phys.* **83,** 33–80 (2011).
6. Jiang, L. *et al.* Quantum Repeater with Encoding. *Phys. Rev. A* **79,** 32325 (2009).
7. Munro, W. J., Harrison, K. A., Stephens, A. M., Devitt, S. J. & Nemoto, K. From quantum multiplexing to high-performance quantum networking. *Nature Photon.* **4,** 792–796 (2010).
8. Fowler, A. G. *et al.* Surface code quantum communication. *Phys. Rev. Lett.* **104,** 180503 (2010).
9. Muralidharan, S., Kim, J., Lütkenhaus, N., Lukin, M. D. & Jiang, L. Ultrafast and Fault-Tolerant Quantum Communication across Long Distances. *Physical Review Letters* **112,** 250501 (2014).
10. Muralidharan, S., Zou, C. L., Li, L., Wen, J. & Jiang, L. Overcoming erasure errors with multilevel systems. *arxiv:/1504.08054v1* (2015).
11. Stace, T. M., Barrett, S. D. & Doherty, A. C. Thresholds for Topological Codes in the Presence of Loss. *Phys. Rev. Lett.* **102,** 200501–200504 (2009).
12. Deutsch, D. *et al.* Quantum privacy amplification and the security of quantum cryptography over noisy channels. *Phys. Rev. Lett.* **77,** 2818–2821 (1996).
13. Dür, W., Briegel, H. J., Cirac, J. I. & Zoller, P. Quantum repeaters based on entanglement purification. *Phys. Rev.* **A 59,** 169–181 (1999).
14. Munro, W., Azuma, K., Tamaki, K. & Nemoto, K. Inside Quantum Repeaters. *IEEE Jour. Selected topics in Quantum electronics* **21,** 1–13 (2015).
15. Zukowski, M., Zeilinger, A., Horne, M. A. & Ekert, A. K. Event-ready-detectors Bell experiment via entanglement swapping. *Phys. Rev. Lett.* **71,** 4287 (1993).
16. Bonarota, M., Gouet, J. L. L. & Chaneliere, T. Highly multimode storage in a crystal. *New J. Phys.* **13,** 13013 (2011).
17. Zwerger, M., Briegel, H. J. & Dür, W. Hybrid architecture for encoded measurement-based quantum computation. *Scientific reports* **4,** 5364 (2014).
18. Nielsen, M. A. & Chuang, I. *Quantum computation and quantum information* (Cambridge University Press, Cambridge, UK; New York, 2000).
19. Gottesman, D. & Chuang, I. L. Demonstrating the viability of universal quantum computation using teleportation and single-qubit operations. *Nature* **402,** 390 (1999).
20. Jiang, L., Taylor, J. M., Sorensen, A. S. & Lukin, M. D. Distributed Quantum Computation Based-on Small Quantum Registers. *Phys. Rev. A* **76,** 62323 (2007).
21. Munro, W. J., Stephens, A. M., Devitt, S. J., Harrison, K. A. & Nemoto, K. Quantum communication without the necessity of quantum memories. *Nature Photonics* **6,** 777–781 (2012).
22. Ralph, T. C., Hayes, A. J. F. & Gilchrist, A. Loss-tolerant optical qubits. *Phys. Rev. Lett.* **95,** 100501 (2005).
23. Jiang, L., Taylor, J. M., Khaneja, N. & Lukin, M. D. Optimal approach to quantum communication algorithms using dynamic programming. *Proc. Natl. Acad. Sci. USA.* **104,** 17291–17296 (2007).
24. Bratzik, S., Kampermann, H. & Bruss, D. Secret key rates for an encoded quantum repeater. *Phys. Rev. A* **89,** 32335 (2014).
25. Bennett, C. H., DiVincenzo, D. P. & Smolin, J. A. Capacities of Quantum Erasure Channels. *Phys. Rev. Lett.* **78,** 3217–3220 (1997).
26. Knill, E. Quantum computing with realistically noisy devices. *Nature* **434,** 39–44 (2005).
27. Ewert, F., Bergmann, M. & van Loock, P. Ultrafast Long-Distance Quantum Communication with Static Linear Optics. *arxiv:/1503.06777* (2015).
28. Azuma, K., Tamaki, K. & Lo, H.-K. All-photonic quantum repeaters. *Nature comm.* **6,** 6787 (2015).
29. Hosseini, M., Sparkes, B. M., Campbell, G., Lam, P. K. & Buchler, B. C. High efficiency coherent optical memory with warm rubidium vapour. *Nature Commun.* **2,** 174 (2011).
30. Chen, Y.-H. *et al.* Coherent Optical Memory with High Storage Efficiency and Large Fractional Delay. *Phys. Rev. Lett.* **110,** 83601 (2013).
31. Duan, L. M., Lukin, M. D., Cirac, J. I. & Zoller, P. Long-distance quantum communication with atomic ensembles and linear optics. *Nature* **414,** 413–418 (2001).

32. Lukin, M. D. *et al.* Dipole blockade and quantum information processing in mesoscopic atomic ensembles. *Phys. Rev. Lett.* **87,** 37901 (2001).
33. Peyronel, T. *et al.* Quantum nonlinear optics with single photons enabled by strongly interacting atoms. *Nature* **488,** 57–60 (2012).
34. Monroe, C. & Kim, J. Scaling the ion trap quantum processor. *Science* **339,** 1164–1170 (2013).
35. Chiaverini, J. *et al.* Realization of quantum error correction. *Nature* **432,** 602 (2004).
36. Nigg, D. *et al.* Quantum computations on a topologically encoded qubit. *Science* **345,** 302–305 (2014).
37. Waldherr, G. *et al.* Quantum error correction in a solid-state hybrid spin register. *Nature* **506,** 204–207 (2014).
38. Medford, J. *et al.* Quantum-Dot-Based Resonant Exchange Qubit. *Phys. Rev. Lett.* **111,** 50501 (2013).
39. Bernien, H. *et al.* Heralded entanglement between solid-state qubits separated by three metres. *Nature* **497,** 86–90 (2013).
40. Togan, E. *et al.* Quantum entanglement between an optical photon and a solid-state spin qubit. *Nature* **466,** 730–734 (2010).
41. Bernien, H. *et al.* Heralded entanglement between solid-state qubits separated by three metres. *Nature* **497,** 86–90 (2013).
42. De Greve, K. *et al.* Quantum-dot spin-photon entanglement via frequency downconversion to telecom wavelength. *Nature* 491, 421–425 (2012).
43. Kim, T., Maunz, P. & Kim, J. Efficient collection of single photons emitted from a trapped ion into a single-mode fiber for scalable quantum-information processing. *Phys. Rev. A* **84,** 063423 (2011).
44. Casabone, B. *et al.* Enhanced Quantum Interface with Collective Ion-Cavity Coupling. *Phys. Rev. Lett.* **114,** 023602 (2015).
45. Meyer, H. M. *et al.* Direct Photonic Coupling of a Semiconductor Quantum Dot and a Trapped Ion. *Phys. Rev. Lett.* **114,** 123001 (2015).
46. Tiecke, T. G. *et al.* Nanophotonic quantum phase switch with a single atom. *Nature* **508,** 241–244 (2014).
47. Shomroni, I. *et al.* All-optical routing of single photons by a one-atom switch controlled by a single photon. *Science* **345** 903–906 (2014).
48. Bagci, T. *et al.* Optical detection of radio waves through a nanomechanical transducer. *Nature* **507,** 81–85 (2014).
49. Andrews, R. W. *et al.* Bidirectional and efficient conversion between microwave and optical light. *Nature Phys*. **10,** 321–326 (2014).
50. Devoret, M. H. & Schoelkopf, R. J. Superconducting Circuits for Quantum Information: An Outlook. *Science* **339,** 1169–1174 (2013).
51. Kómár, P. *et al.* A quantum network of clocks. *Nature Phys*. **10,** 582–587 (2014).
52. Gottesman, D., Jennewein, T. & Croke, S. Longer-baseline telescopes using quantum repeaters. *Phys. Rev. Lett.* **109,** 070503 (2012).
53. Monroe, C. *et al.* Large-scale modular quantum-computer architecture with atomic memory and photonic interconnects. *Phys. Rev. A* **89,** 22317 (2014).
54. Kimble, H. J. The quantum internet. *Nature* (*London*) **453,** 1023–1030 (2008).

Acknowledgements

This work was supported by the DARPA Quiness program, ARL CDQI program, ARO, AFOSR, NBRPC (973 program), the Alfred P. Sloan Foundation and the Packard Foundation. We thank Anna Wang, Hong Tang, Ryo Namiki, Prasanta Panigrahi and Steven Girvin for discussions.

Author Contributions

J.K., N.L., M.L. and L.J. conceived the original concept and designed the research project. S.M. and L.L. carried out the theoretical and numerical analysis. S.M., L.L. and L.J. prepared the manuscript with inputs from J.K., N.L. and M.L.

Additional Information

Supplementary information accompanies this paper at http://www.nature.com/srep

Competing financial interests: The authors declare no competing financial interests.

How to cite this article: Muralidharan, S. *et al.* Optimal architectures for long distance quantum communication. *Sci. Rep.* **6**, 20463; doi: 10.1038/srep20463 (2016).